Theoretical Study of Tungsten Carbonyl Complexes (n = 1−6): Structures, Binding Energies, and Implications for Gas Phase Reactivities

ARTICLE *in* THE JOURNAL OF PHYSICAL CHEMISTRY A · MAY 1997

Impact Factor: 2.69 · DOI: 10.1021/jp9639962

3 AUTHORS, INCLUDING:

Philippe Maître
Université Paris-Sud 11
140 PUBLICATIONS **3,546** CITATIONS
SEE PROFILE

Gilles Ohanessian
French National Centre for Scientific Research
115 PUBLICATIONS **3,711** CITATIONS
SEE PROFILE

Theoretical Study of Tungsten Carbonyl Complexes $W(CO)_n^+$ ($n = 1-6$): Structures, Binding Energies, and Implications for Gas Phase Reactivities

Heinz H. Büker,[†,‡] Philippe Maître,*[,§] and Gilles Ohanessian*[,‡]

Laboratoire des Mécanismes Réactionnels, URA 1307-CNRS, Ecole Polytechnique, 91128 Palaiseau Cedex, France, and, Laboratoire de Chimie Théorique, URA 506-CNRS, Université de Paris XI, 91405 Orsay Cedex, France

Received: December 6, 1996; In Final Form: March 7, 1997[⊗]

The electronic structure and geometry of $W(CO)_n^+$ ($n = 1-6$) have been studied at the B3LYP and *ab initio* levels. We find that the ground state of $W(CO)^+$ is linear with a sextet spin state, that a linear sextet and a bent quartet are nearly degenerate for $W(CO)_2^+$, and that doublet states are unambiguously the ground states of $W(CO)_3^+$ to $W(CO)_6^+$. Successive $(CO)_{n-1}W^+-CO$ binding energies have been computed to be larger than any of those previously determined for other transition metals. We compare our results with available experimental data. Electron transfers are very important: (i) σ donation from the CO's to the metal is found to be more favorable when involving 5d rather than 6p leading to a preference for the bent rather than linear structures for $W(CO)_n^+$ ($n = 2-4$); (ii) π back-donation plays a crucial role in shaping these molecules. These effects provide the driving force for the spin changes as the number of ligands increases. Spin lowering is associated with an increasing number of doubly rather than singly occupied $5d_\pi$ metal orbitals, which enhances the back-donation ability while reducing the repulsion between σ metal electrons and CO lone pairs. On the basis of our results, we propose an interpretation of the observed differences in gas phase reactivity of $W(CO)_n^+$ with small hydrocarbons as a function of n. The rationale for this interpretation is that the initially formed $(CO)_nW^+-$(hydrocarbon) complex should either have a ground or a low-lying excited state bearing at least two unpaired electrons on the metal to be able to further activate the hydrocarbon efficiently.

I. Introduction

Transition metal carbonyl complexes are reference molecules in more than one area of inorganic chemistry. Binding in such highly symmetrical molecules has been a valuable testing ground for the donation/back-donation model of metal−ligand interaction. This has resulted in a synergistic development of theoretical models and spectroscopic studies up to a rather sophisticated level, including part of the vibrational progressions.[1] Interest in $W(CO)_6$ is also due in part to the fact that it is a very common material in solution phase organometallic chemistry,[2] where displacement of CO by several types of ligands is readily accomplished.[3] In the last decade, the corresponding cation $W(CO)_6^+$ has become a reference molecule in mass spectrometry (MS). Many MS studies involve activation steps aimed at dissociating ions (in order, e.g., to derive structural information from the nature of the fragments formed), and a crucial aspect of these methods is the amount of energy actually deposited in the parent species. In cases such as metal carbonyls, where all fragmentation processes (or nearly so) are simple bond cleavages, knowledge of the successive $(CO)_{n-1}W^+-CO$ binding energies enables one to derive distributions of internal energies on the basis of the relative intensities of $W(CO)_n^+$ fragments ($0 \le n \le 6$). This has lead to a wealth of information about several activation processes such as low- and high-energy collision-induced dissociation (CID),[4] electron-induced dissociation (EID),[5] neutralization−reionization (NRMS),[6] and charge exchange processes.[7] These analyses rely on binding energies which have been obtained as appearance potentials for the successive $W(CO)_n^+$ fragments, when neutral $W(CO)_6$ is subjected to the impact of accelerated electrons.[8] However there is an important scatter of binding energies in the literature, and accurate values are clearly desirable.

In recent years a large body of data has begun to accumulate for the successive metal−carbonyl binding energies in cationic complexes. The main techniques used are threshold CID in an ion beam instrument,[9] threshold photoelectron−photoion coincidence (TPEPICO),[10] and quantum chemical calculations.[11] Nearly all of these studies have dealt with first-row transition metals, so that detailed results on the entire row are now available for mononuclear carbonyl complexes. Data for second- and third-row metal carbonyls remain quite scarce, so that there is a strong need to extend these studies to heavier elements.

Ion−molecule reactions of $W(CO)_n^+$ ($n = 0-4$) with small hydrocarbons have recently been carried out,[12] and it was found that the reactivity strongly depends upon the number of carbonyl ligands on the metal. For instance methane activation leading to the formation of metal−methylene complexes through H_2 elimination is observed for $n = 0-2$ but not for $n = 3$ or 4. Another important variation, especially prominent in the reactions with alkenes, is the participation of CO detachment to the reactivity. Thus, in the reactions with propene, elimination of $H_2 + CO$ is exclusively observed with WCO^+, the same channel is dominant with $W(CO)_2^+$ but is accompanied by minor amounts of losses of $2H_2$ and of CO,$W(CO)_3^+$ leads essentially to loss of H_2, with a minor competitive loss of CO, and the latter (which is a simple ligand displacement reaction) is the exclusive channel with $W(CO)_4^+$. Understanding these variations requires a knowledge of the metal−carbonyl binding energies, but perhaps more importantly an understanding of the electronic structure of all $W(CO)_n^+$, including the ground and

[†] Laboratoire des Mécanismes Réactionnels.
[‡] Present address: Institute of Mass Spectrometry, University of Amsterdam, 1018 WS Amsterdam, The Netherlands.
[§] Laboratoire de Chimie Théorique. e-mail: maitre@cth.u-psud.fr.
[⊗] Abstract published in *Advance ACS Abstracts,* April 15, 1997.

S1089-5639(96)03996-5 CCC: $14.00

low-lying excited electronic states. Since W^+ has a sextet ground state[13] and $W(CO)_6^+$ has a doublet ground state, there must be two spin changes along the way. An important feature to determine in the $W(CO)_n^+$ series is the position of these spin changes. The observed reactivity may also be influenced by the geometry of the various ions and the relative energy of excited states of the same or other spin multiplicity. This has constituted an additional motivation to undertake a thorough theoretical study of $W(CO)_n^+$ ($n = 1-6$), which is the purpose of the present paper.

Details of the methods used are given in section II. A detailed description of the different electronic states of each complex in their B3LYP optimized geometries is given in section III. In section IV, we compare our B3LYP and ab initio results, and a comparison of our results to literature data is given in section V. Finally, we attempt to relate computational results to experimental observations in section VI.

II. Theoretical Methods

Low-energy structures of the successive $W(CO)_n^+$ ($n = 1-6$) complexes in different spin states (sextet, quartet, and doublet) have been characterized using the density functional approach. Structures were fully characterized (geometries and harmonic frequencies) using a hybrid density functional denoted as B3LYP,[14] which is a modified version of a hybrid functional originally proposed by Becke.[15] Even though this hybrid density functional has been shown to perform well for various transition metal containing systems,[16] results for a selected set of complexes were compared to those obtained using ab initio post-HF methods, where all valence plus the metal outer core $5s^2$ and $5p^6$ electrons were correlated. Post-HF calculations were based on second-order Moller−Plesset perturbation (MP2) formalism and also, for the smaller complexes, the coupled-cluster formalism with the singles and doubles substitutions (CCSD)[17] and a perturbational estimate of the connected triples (CCSD(T)).[18] It should be noted that while the spin contamination is rather small at the B3LYP level (the error on the $\langle S^2 \rangle$ is less than 15×10^{-3} for all the states considered), it is significant at the UMP2 level (the largest error on the $\langle S^2 \rangle$ is 3×10^{-2} for the sextet and doublet and 6×10^{-2} for a quartet).

A small basis set (basis 1) was used to expand the Kohn−Sham orbitals, and two larger bases (2 and 3) were also used for the post-HF calculations. In all calculations, the 60 inner-core electrons of W were described by a relativistic effective core potential.[19] In basis 1, W (5s, 5p, and valence electrons) was described by an optimized [4s4p3d] contraction of a (7s6p5d) Gaussian basis set[20] and the C and O atoms were represented by the polarized full double-ζ set of Dunning and Hay.[21] In order to describe electron correlation at the post-HF levels, basis set extensions were made by adding (1) one set of f polarization functions ($\zeta_f = 0.225$) to W (basis 2) and (2) two f polarization functions ($\zeta_f = 0.225, 0.700$) to W and extending the CO basis set to cc-pVTZ[22] (basis 3). Cartesian representation of the d and f spaces has been used for all the calculations. Finally, we tested the effect of adding diffuse sp functions on C and O in some cases (see section IV).

The Gaussian 92/DFT and Gaussian 94 packages[23] have been used throughout. Harmonic frequencies have been determined at the B3LYP level. When mentioned in the text, population analyses refer to results obtained with the Weinhold formalism (natural population analysis)[24] included in the Gaussian packages.

III. Discussion of the B3LYP Results

Results. B3LYP results for the low-lying states of $W(CO)_n^+$ ($n = 1-6$) are listed in Table 1. Binding energies of $W(CO)_n^+$ were calculated with respect to the lowest B3LYP $W(CO)_{n-1}^+ + CO$ dissociation limit. All the listed structures have been characterized as being minima, and the figure labels in Table 1 refer to the corresponding molecular frame orientation given in Figure 1. Assuming this molecular orientation, we give in Table 1 the main geometrical parameters and the W^+ electronic configuration for each complex structure. As expected, the spin multiplicity of the ground state decreases as the number of CO ligands increases, and our B3LYP results suggest that $W(CO)^+$, $W(CO)_2^+$, and $W(CO)_n^+$ ($n = 3-6$) have a sextet, quartet, and doublet ground state respectively. $W(CO)^+$ has a linear geometry. $W(CO)_2^+$ has a bent shape (**2b**) in its $^4B_2$ B3LYP ground state but a linear geometry (**2a**) in its $^6\Sigma$ excited state. As discussed in section IV, these two states are predicted to be very close at the post-HF level. $W(CO)_3^+$ has a trigonal pyramid geometry (**3c**) in its $^2A'$ ground state but rather prefers planar (**3a** or **3b**) geometries in its excited sextet and quartet states. $W(CO)_4^+$ has a butterfly shape (**4c**) in its $^2A_1$ ground state and square pyramidal one (**4a** or **4b**) in its quartet excited states. $W(CO)_5^+$ has a square pyramid geometry (**5c**) in its $^2B_1$ ground state, but both square pyramid (**5b**) and trigonal bipyramid (**5a**) structures have been characterized on the quartet potential energy surfaces. $W(CO)_6^+$ has a slightly distorted structure (**6**) in its $^2B_{2g}$ ground state.

Overview of the Bonding in $W(CO)_n^+$. In order to help clarify the following discussion on the geometrical and electronic structures of each complex, we would like first to give a brief outline to aid in understanding the electronic configuration in the lowest-lying states of each case and especially the spin changes from sextet to quartet to doublet as the number of CO increases. The ground state of W^+ is a sextet ^6D ($6s^15d^4$), with a first excited state ^6S ($5d^5$) only 9.5 kcal/mol higher in energy, but with very high-lying quartet and doublet states.[13] Therefore, sd hybridization, which amounts to $^6D/^6S$ mixing on the metal, is easily realized, while the two successive spin changes, when going from W^+ to $W(CO)_5^+$, must be induced by the increasing ligand field.

As can be seen in Table 1, the ∠CWC angles of the ground state of each complex are all roughly equal to either 90° or 180°, and therefore, the electronic configuration on the metal cation can be simply understood by considering that the CO ligands bind to W^+ along three perpendicular axes. One can therefore distinguish, as in the well-known octahedral coordination case, two subsets of d orbitals on W^+: assuming that the metal−ligand bonds are along the *x*, *y*, and *z* axes, there are (i) two d orbitals ($d_{x^2-y^2}$,d_{z^2}) pointing toward the ligands (d_σ) which are symmetry adapted for the ligand-to-metal σ electron transfer and (ii) the three others (d_{xy}, d_{xz}, d_{yz}) with two nodes along the metal−ligands planes (d_π) which are symmetry adapted for the metal-to-ligand π electron transfer (back-donation). Thus, as the number of ligands increases, the sextet spin coupling on the metal is less and less favorable since it leads to electron repulsions between singly occupied d_σ orbitals and σ CO lone pairs. These three-electron repulsions can be reduced by an sd hybridization of the singly occupied d_σ orbital (Scheme 1) but this is only efficient in the smaller complexes (as we will see in the sextet states of $W(CO)^+$ and $W(CO)_2^+$). For larger complexes, it is more favorable to promote the metal to a high-energy electronic configuration by successively transferring the two d_σ electrons into d_π orbitals, which strengthens the W−CO

TABLE 1: B3LYP Binding Energies (in kcal/mol) and Main Geometrical Parameters (Bond Lengths in Å, Angles in deg) for a Selected Set of $W(CO)_n^+$ States

system	shape	symmetry	figure label[a]	W^+ electronic configuration[b]	state	∠CWC[c,d]		W−C[d]		C−O[d]	D_e[e]
CO					$^1\Sigma$					1.14	
$W(CO)^+$	linear	$C_{\infty v}$		$(\sigma,z^2)^1(\pi,xz,yz)^2(\delta,x^2-y^2,xy)^2$	$^6\Sigma$				2.04	1.14	**53.8**
				$(\sigma,z^2)^1(\pi,xz,yz)^3(\delta,x^2-y^2,xy)^1$	$^4\Phi$				1.94	1.15	34.3
				$(\sigma,z^2)^1(\pi,xz,yz)^4$	$^2\Sigma$				1.89	1.16	3.4
$W(CO)_2^+$	linear	$D_{\infty h}$	**2a**	$(\sigma,z^2)^1(\pi,xz,yz)^2(\delta,x^2-y^2,xy)^2$	$^6\Sigma$				2.17	1.14	38.6
				$(\sigma,z^2)^1(\pi,xz,yz)^3(\delta,x^2-y^2,xy)^1$	$^4\Phi$				2.09	1.14	23.8
				$(\pi,xz,yz)^4(\delta,x^2-y^2,xy)^1$	$^2\Delta$				2.05	1.15	3.9
	bent	C_{2v}	**2b**	$(b_1,xz)^1(a_2,xy)^2(a_1,z^2-y^2)^1(a_1,y^2)^1$	$^4B_1$		107.1		2.00	1.15	24.7
				$(b_1,xz)^2(a_2,xy)^1(a_1,z^2-y^2)^1(a_1,y^2)^1$	$^4A_2$		77.0		1.98	1.15	27.0
				$(b_1,xz)^1(a_2,xy)^1(a_1,z^2-y^2)^2(a_1,y^2)^1$	$^4B_2$		87.7		1.97	1.15	**45.8**
				$(b_1,xz)^2(a_2,xy)^2(a_1,z^2-y^2)^1$	$^2A_1$		89.8		1.95	1.16	17.1
				$(b_1,xz)^1(a_2,xy)^2(a_1,z^2-y^2)^2$	$^2B_1$		99.2		1.95	1.15	26.8
				$(b_1,xz)^2(a_2,xy)^1(a_1,z^2-y^2)^2$	$^2A_2$		80.3		1.94	1.15	29.0
$W(CO)_3^+$	planar	D_{3h}	**3a**	$(a_1',z^2)^1(e',xy,x^2-y^2)^2(e'',xz,yz)^2$	$^6A_1'$				2.12	1.14	21.3
		C_{2v}	**3b**	$(b_2,yz)^2(b_1,xz)^1(a_2,xy)^1(a_1,y^2)^1$	$^4B_2$		91.2	*(1)*	1.98	1.15	41.9
								(2)	2.11	1.14	
		C_{2v}	**3b**	$(b_2,yz)^1(b_1,xz)^2(a_2,xy)^2$	$^2B_2$		93.0	*(1)*	1.95	1.16	15.2
								(2)	2.10	1.14	
		C_{2v}	**3b**	$(b_2,yz)^2(b_1,xz)^2(a_2,xy)^1$	$^2A_2$		90.4	*(1)*	1.92	1.16	21.8
								(2)	2.11	1.14	
		C_{2v}	**3b**	$(b_2,yz)^2(b_1,xz)^1(a_2,xy)^2$	$^2B_1$		91.8	*(1)*	1.98	1.15	26.6
								(2)	2.06	1.15	
	trigonal pyramid	C_s	**3c**	$(a')^2(a')^2(a'')^1$	$^2A''$	*(1,1)*	90.7	*(1)*	1.98	1.15	48.7
						(1,2)	83.0	*(2)*	1.95	1.15	
		C_s	**3c**	$(a')^2(a')^1(a'')^2$	$^2A'$	*(1,1)*	83.9	*(1)*	1.96	1.15	**49.6**
						(1,2)	96.3	*(2)*	1.97	1.15	
$W(CO)_4^+$	square planar	D_{4h}	**4a**	$(a_{1g},z^2)^1(e_g,xz,yz)^2(b_{1g},xy)^1(a_{2u})^1$	$^6B_{1u}$				2.14	1.15	14.6
		D_{4h}	**4a**	$(a_{1g},z^2)^1(e_g,xz,yz)^2(b_{1g},xy)^2$	$^4A_{1g}$				2.12	1.14	34.1
		D_{4h}	**4a**	$(e_g,xz,yz)^4(b_{1g},xy)^1$	$^2B_{2g}$				2.10	1.15	8.9
		D_{2h}	**4b**	$(b_{1g},xy)^2(b_{2g},xz)^1(b_{3g},yz)^2$	$^2B_{2g}$			*(1)*	2.06	1.15	19.9
								(2)	2.12	1.14	
	butterfly	C_{2v}	**4c**	$(b_2,yz)^1(a_1,z^2)^2(a_2,xy)^2$	$^2B_2$	*(1,1)*	177.2	*(1)*	2.12	1.14	39.3
						(2,2)	97.0	*(2)*	1.97	1.15	
		C_{2v}	**4c**	$(b_2,yz)^2(a_1,z^2)^2(a_2,xy)^1$	$^2A_2$	*(1,1)*	176.3	*(1)*	2.12	1.14	41.2
						(2,2)	83.3	*(2)*	1.96	1.15	
		C_{2v}	**4c**	$(b_2,yz)^2(a_1,z^2)^1(a_2,xy)^2$	$^2A_1$	*(1,1)*	175.0	*(1)*	2.07	1.15	**42.9**
						(2,2)	84.7	*(2)*	1.99	1.15	
$W(CO)_5^+$	trigonal bipyramid	C_{2v}	**5a**	$(b_2,yz)^2(b_1,xz)^1(a_2,xy)^1(a_1,z^2)^1$	$^4B_2$	*(1,2)*	87.3	*(1)*	2.06	1.15	19.5
						(1,3)	129.9	*(2)*	2.11	1.14	
								(3)	2.11	1.14	
	square pyramid	C_{4v}	**5b**	$(e,xz,yz)^2(b_2,xy)^2(a_1,z^2)^1$	$^4A_1$	*(1,2)*	105.3	*(1)*	2.13	1.14	20.0
								(2)	2.09	1.15	
		C_{4v}	**5b**	$(e,xz,yz)^4(b_2,xy)^1$	$^2B_2$	*(1,2)*	90.8	*(1)*	1.96	1.15	38.0
								(2)	2.12	1.14	
		C_{2v}	**5c**	$(b_2,yz)^2(b_1,xz)^1(a_2,xy)^2$	$^2B_1$	*(1,2)*	91.6	*(1)*	1.99	1.15	**42.2**
						(1,3)	92.9	*(2)*	2.08	1.15	
								(3)	2.12	1.14	
$W(CO)_6^+$	pseudo octahedral	D_{4h}	**6**	$(e_g,xz,yz)^4(b_{2g},xy)^1$	$^2B_{2g}$			*(1)*	2.08	1.15	**42.0**
								(2)	2.12	1.14	

[a] Figure labels refer to the ones given in Figure 1. [b] This is a simplified description corresponding to the main $W^+(d^5)$ electronic configuration and therefore neglecting hybridization on the metal and delocalization on the ligands. [c] ∠WCO angles are not given since they are always very close to 180°. [d] When there are different classes of symmetry equivalent CO's (see Figure 1), (*i*, *j*) refers to the $\angle C_iWC_j$ angles. (*i*) refers to the WC_i and C_iO_i bond lengths. [e] The values for the ground states are given in boldface.

bonds since it (i) reduces the σ repulsion and favors the ligand-to-metal σ donation and (ii) increases the potential metal-to-ligand π electron transfers from doubly instead of singly occupied d_π orbitals into the antibonding π carbonyl orbitals.

The participation of the valence p orbitals of the metal is questionable in cationic organometallic systems. Indeed, in the case of W^+ for example, atomic states with a nonzero 6p occupation are known to be high in energy.[13] Thus, in a first approximation, we can consider that only the 6s and the two $5d_\sigma$ orbitals are available to get the donation from the CO σ lone pairs, while occupying the $5d_\pi$ will contribute to the metal-to-ligand donation. With the discussion of $W(CO)^+$ and $W(CO)_2^+$, we will refine this simplified view of the bonding and define precisely, in particular, to what extent the 6p orbitals participate to the bonding in polarizing the metal σ and π orbitals. For $W(CO)_3^+$ and larger complexes, we will present the results based on the fact that doublet states are the most stable and show that the state ordering for a given spin coupling on the metal is governed by the extent of metal-to-ligand π donation.

W^+. The experimental energy difference between the *J*-weighted average energies of the ^6D ($6s^1\,5d^4$) W^+ ground state and the first excited state ^6S ($5d^5$) is 9.5 kcal/mol.[13] A good description of this energy splitting is a prerequirement for the study of $W(CO)_n^+$ complexes where 6s−5d hybridization,

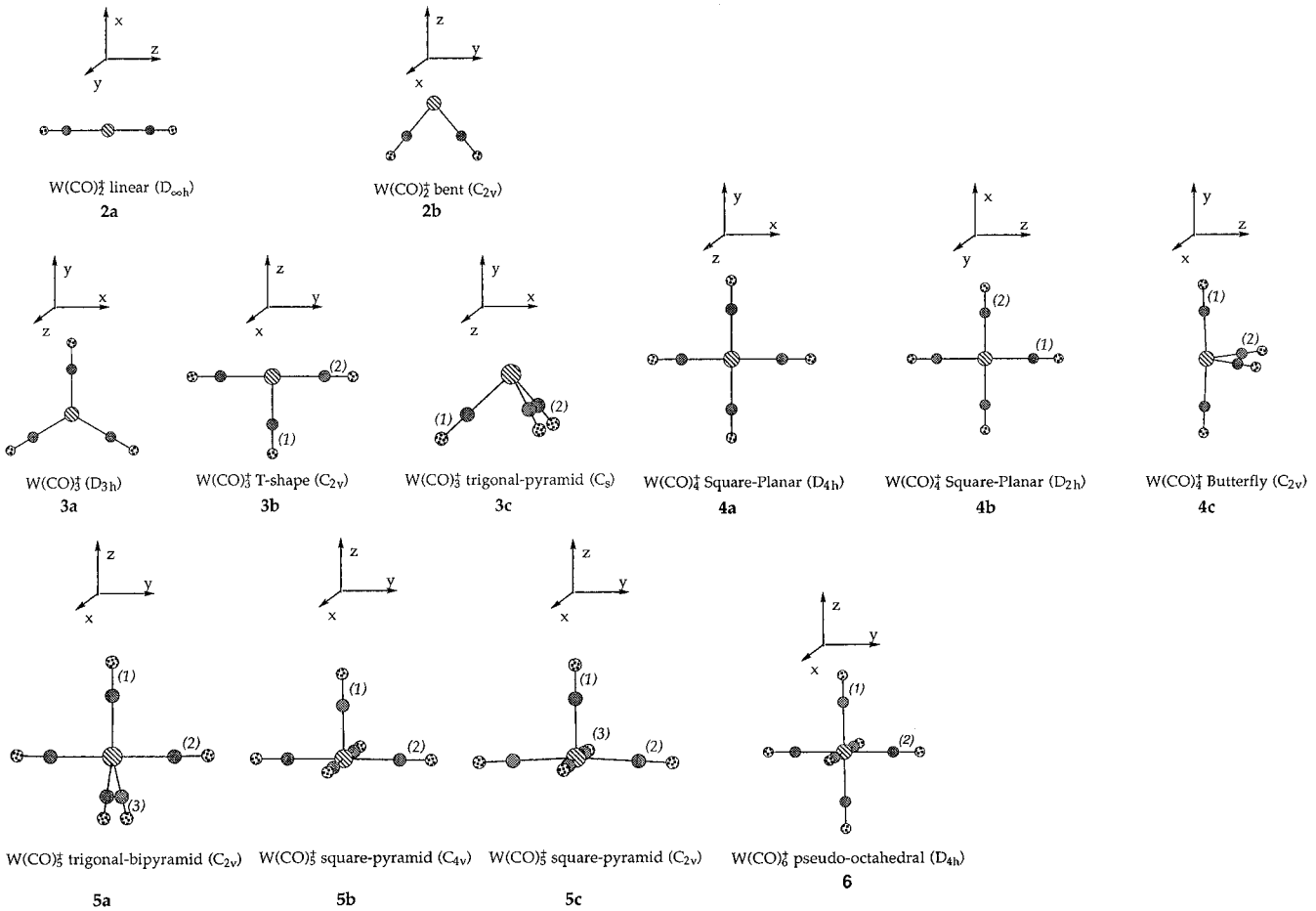

Figure 1. Structure shape and corresponding symmetry point group of the different isomers of each $W(CO)_n^+$ complex optimized at the B3LYP level. Labels (*i*) specify the different classes of symmetry equivalent CO's. Bond lengths and angles are given in Table 1.

SCHEME 1: Valence σ Molecular Orbitals of $W(CO)^+$

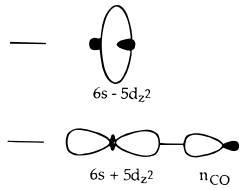

which corresponds to the mixing of the two above mentioned states on W^+, plays an important role in the bonding. Using our smallest basis set (basis 1), the B3LYP value of the W^+ ($^6D-^6S$) energy splitting is 12.1 kcal/mol, in reasonable agreement with the experimental value. This is also the case of the UHF level, with a splitting of 12.7 kcal/mol. While the inclusion of electron correlation, which is expected to be slightly larger in a $5d^5$ than in a $6s^15d^4$ electronic configuration, should lower the splitting relative to UHF, we obtain UMP2/1 and CCSD(T)/1 values of 21.3 and 21.2 kcal/mol, respectively. (If the outer core 5s and 5p electrons are not correlated, the $^6D-^6S$ energy splitting is 11.2 kcal/mol at the MP2/2 level. While this could potentially lead to a better description of the sd hybridization, we found that, on the contrary, it leads to a slight reduction of the bond dissociation energies (BDE's) (about −2 kcal/mol for each BDE. Since this approach seems to be flawed, the outer-core electron correlation was maintained.) The addition of a set of f functions on the metal has nearly no effect (basis 2), while the addition of the second set of f functions (basis 3) lowers these values to 16.2 and 16.3 kcal/mol, respectively. In conclusion, one should keep in mind that the s/d hybridization is probably better described at the B3LYP than at the *ab initio* level, which will lead to smaller *ab initio* than B3LYP binding energies in cases involving significant changes in metal s/d hybridization, such as $W(CO)^+$ and quartet $W(CO)_2^+$.

$W(CO)^+$. The linear geometry of each spin state has been optimized for $W(CO)^+$, and we found that the ground state is a $^6\Sigma$. Minimizing σ repulsion leads to singly occupying both d_π (d_{xz} and d_{yz}) and both d_δ orbitals (d_{xy} and $d_{x^2-y^2}$), corresponding to a $^6\Sigma$ state (see Table 1). In the σ space, hybridization between the 6s and $5d_{z^2}$ orbitals helps reducing electron density along the *z* axis (see Scheme 1). This sd hybridization seems to be very efficient (the singly occupied σ on W^+ is 50% 6s and 50% $5d_{z^2}$) to reduce the σ electron repulsion, and it results in a fairly large binding energy of 53.8 kcal/mol at the B3LYP level. Other sextet states are higher in energy since both the s and d_{z^2} orbitals are singly occupied. In such a case, s/d_{z^2} hybridization is no longer operative, leading to high σ electron repulsion with the ligand. The $^4\Phi$ state derives from the $^6\Sigma$ by a promotion of the W^+ σ electron into the d_π set. The shortening of the W−C (1.94 versus 2.04 Å) and lengthening of the C−O (1.15 versus 1.14 Å) bonds indicate, as expected, an increase of electron transfers. Indeed, according to the population analysis of the $^6\Sigma$ and $^4\Phi$ states, there is an electron transfer of about 0.15 and 0.30 electron from a singly and doubly occupied d_π orbital, respectively. Nevertheless, the reinforcement of the W−CO bond is not sufficient to overcome the large promotion energy to a quartet state on W^+, and the B3LYP binding energy of the $^4\Phi$ state relative to the sextet ground state dissociation limit is only 34.2 kcal/mol. This π^3 electronic configuration must give rise to the most stable states among the quartet manifold since it maximizes π occupancy, and therefore metal-to-ligand back-donation. The $^2\Delta$ state derives from the $^4\Phi$ by

SCHEME 2: Back-Donating π Molecular Orbitals of $W(CO)^+$

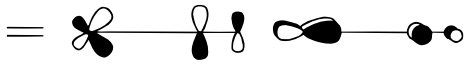

a promotion of one W^+ d_δ electron into the d_π set, and it thereby results in a further shortening of the W−C (1.89 versus 1.94 Å) and lengthening of the C−O (1.16 versus 1.15 Å) bonds. This state is predicted to be slightly bound by 3.4 kcal/mol at the B3LYP level.

$W(CO)_2^+$. As for $W(CO)^+$, all possible spin states have been considered: sextet, quartet, and doublet. Linear (**2a**) and bent (**2b**) isomers have been characterized on the quartet and doublet potential energy surfaces, and the bent structure is the absolute minimum in both cases. On the contrary, no bent extremum was found on the sextet surface. The $W(CO)_2^+$ ground state is delicate to assign because two different spin multiplicities compete and, at our best level of theory, the conclusion is that linear $^6\Sigma$ and bent $^4B_2$ are probably very close in energy (see section IV). The existence of the bent ground state for $M(CO)_2^+$ is rare. In a systematic study of all first and second-row transition metal dicarbonyl complexes, Barnes et al. found that all are linear except $Mn(CO)_2^+$.[11b]

The $W(CO)_2^+$ $^6\Sigma$ state can be deduced from the $^6\Sigma$ ground state of $W(CO)^+$ by adding the second ligand on the opposite side of the metal. In $W(CO)^+$, there are two types of hybridization on the metal. (i) The sd hybridization, which reduces the σ metal−ligand repulsion by removing electron density from the bonding axis, therefore also benefits the second ligand. For an essentially pure σ donor such as H_2O, it may lead to a larger binding energy for the second than for the first ligand. (ii) There might also be, in the case of π acceptor ligands, a polarization of the d_π orbitals toward the first ligand through d_π/p_π mixing (Scheme 2). In $W(CO)_2^+$ the π orbitals are symmetrical, so that this polarization is lost, and this will have the tendency to reduce the binding energy of the second ligand like in linear $W(CO)_2^+$. In the case of $W(CO)_2^+$, the second effect is stronger than the first and it results in a smaller binding energy for the second than for the first ligand. The binding energy of the $^6\Sigma$ state of $W(CO)_2^+$ is 38.6 kcal/mol at the B3LYP level, 15.2 kcal/mol smaller than that of the $^6\Sigma$ ground state of $W(CO)^+$. This loss of binding energy is probably exaggerated at the B3LYP level, which is known to overestimate the first binding energy to an atom,[16] and we indeed found that it is only 8 kcal/mol at our best *ab initio* level (see section IV). This, of course, also has geometrical effects, and one can see in Table 1 that W−C and C−O distances increase and decrease, respectively, when going from $W(CO)^+$ to $W(CO)_2^+$ on the sextet PES.

Linear quartet and doublet states were also considered. As for the sextet, their electronic structures are derived straightforwardly from those of the quartet and doublet states of $W(CO)^+$. Because of the high promotion energy to lower spin states of W^+, the ordering remains sextet < quartet < doublet. However, the back-donating ability of the doubly occupied orbital(s) is now directed toward two ligands simultaneously instead of only one in $W(CO)^+$, leading to much smaller energy differences between various spin states in $W(CO)_2^+$ compared to $W(CO)^+$. In comparing the linear $W(CO)^+$ and $W(CO)_2^+$ geometrical parameters for the quartet and doublet states, an evolution of the bond lengths can be found which is very similar to the one discussed above for the sextet states.

On the quartet PES, three bent minima have been found to be lower in energy than the lowest linear structure corresponding to the $^4\Phi$ state. This structural preference is likely to be due to σ effects. In both linear and bent conformations the in-phase combination of the CO lone pairs donates into a 6s−5d hybrid. However, as can be seen in Scheme 3, the out-of-phase combination of the CO lone pairs is symmetry adapted to interact only with a W^+ 6p in the linear geometry, while in the bent one, it interacts with the empty good σ acceptor 5d orbital and also the 6p. Population analysis of the $^4B_2$ state shows that the electron transfer into the σ acceptor $5d_{yz}$ orbital is large (0.6 electron), which also allows a better π metal-to-ligand electron transfer. Such a preference for the donation into a metal d instead of a p orbital is also at the origin of the distortion in a d^0 ML_6 such as WH_6.[25] In the case of the sextet state where no empty d orbital is available, a scan on the potential energy surface showed that there is no bent extremum.

SCHEME 3: Donation from the Antisymmetric Linear Combination of σ_{CO} in $W(CO)_2^+$: Difference between the Linear and Bent Structures

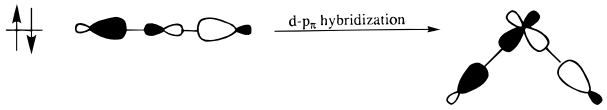

SCHEME 4: Electronic Configurations of the Back-donating π Molecular Orbitals in the Quartet and Doublet States of Bent $W(CO)_2^+$

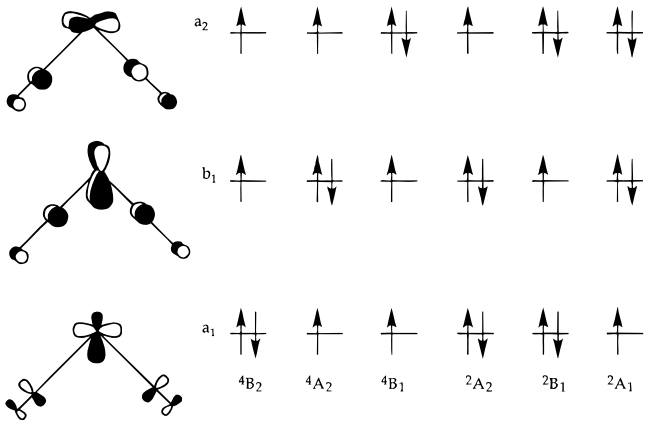

At the B3LYP level, we found that the $^4B_1$ and $^4A_2$ states are almost degenerate and lie about 20 kcal/mol above the $^4B_2$ ground state (see Table 1). This energy ordering demonstrates the importance of maximizing the occupation of the d_π orbitals that have the largest overlap with a maximum of π^*_{CO} orbitals. In the bent geometry, three d_π orbitals are symmetry adapted to interact with linear combinations of π^*_{CO} as depicted in Scheme 4. Assuming a ∠CWC angle of 90°, the $d_\pi - \pi^*_{CO}$ overlap is maximum in the in-plane a_1 MO, and about the same in the out-of-plane a_2 and b_1 ones. Thus the $^4B_2$ ground state corresponds to the double occupancy of the a_1 MO, which maximizes metal-to-ligand donation, and the $^4B_1$ and $^4A_2$ states are of the same energy. The differences in ∠CWC equilibrium angle for these three states (see Table 1) can also be understood using the MO pictures of Scheme 4. Ligand-to-metal donation from the out-of-phase combination of the CO lone pairs is maximum for a ∠CWC right angle (Scheme 4) while the $d_\pi - \pi^*_{CO}$ overlap in the out-of-plane b_1 (a_2) MO increases when the equilibrium angle is smaller (larger) than 90°, and this leads to 77.0° and 107.0° equilibrium angles for the $^4A_2$ and $^4B_1$ states where these orbitals are doubly occupied respectively. On the contrary, since $d_\pi - \pi^*_{CO}$ overlap in the in-plane a_1 MO is maximum for a right angle, the $^4B_2$ ∠CWC equilibrium angle is found to be 89.7°.

SCHEME 5: Electronic Configurations of the Back-Donating π Molecular Orbitals in the Doublet States of Trigonal Pyramidal $W(CO)_3^+$

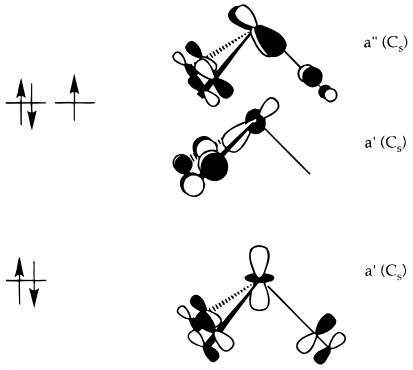

The energy ordering ($^2A_2 \approx {}^2B_1 \ll {}^2A_1$) and ∠CWC equilibrium angles (80.3°, 99.2°, and 89.8°) of the three bent doublet states can also be understood on the basis of the MO pictures of Scheme 4. In the lowest two states, a deviation from the ∠CWC right angle allows an increase of the overlap in one of the doubly occupied linear combination of d_π and π^*_{CO}. Finally, since the $d_\pi - \pi^*_{CO}$ overlap in the out-of-plane b_1 (a_2) MO increases when the equilibrium angle is smaller (larger) than 90°, it is not surprising that the ∠CWC equilibrium angle of the $^2A_1$ was found to be close to a right angle (89.8°).

$W(CO)_3^+$. $W(CO)_3^+$ has a $^2A'$ ground state, and the corresponding minimum energy structure has a trigonal pyramidal shape (**3c**). The binding energy of this state, calculated with respect to the bent $W(CO)_2^+$ $^4B_2$ + CO dissociation limit, is 49.6 kcal/mol (see Table 1). At the same level of theory, the binding energy of the lowest quartet state ($^4B_2$) is also quite large (41.9 kcal/mol). This spin state ordering has been confirmed using *ab initio* approaches, and our best estimate for this state energy splitting is at least 7 kcal/mol (see section IV). This spin change is not surprising if one considers the evolution of the relative energies of the three spin states from $W(CO)^+$ to $W(CO)_2^+$. From the B3LYP results on $W(CO)_2^+$, one can extract the binding energy of CO to $W(CO)^+$ in a sextet, quartet, and doublet spin state as 38.6, 65.3, and 79.4 kcal/mol, respectively. The relative energies of these three spin states in $W(CO)_2^+$ are +7.2 ($^6\Sigma$), 0.0 ($^4B_2$), and +16.8 ($^2A_2$) kcal/mol, respectively. Assuming that the binding energy in each spin state is roughly the same in $W(CO)_2^+$ and $W(CO)_3^+$, one would have expected to have the doublet and quartet states close in energy for $W(CO)_3^+$, with a sextet state about 30 kcal/mol higher in energy. This is close to our B3LYP results where the lowest sextet and quartet states are respectively 28.3 and 7.7 kcal/mol higher in energy than the doublet ground state.

As discussed in the beginning of this section, ∠CWC angles in all $W(CO)_n^+$ ground states are close to 90° or 180°, and this is largely due to the maximization of back-donating interactions. In doublet states such as the ground state of $W(CO)_3^+$, there are two doubly occupied metal d orbitals which efficiently donate electrons to π^*_{CO} orbitals. In order to maximize this type of interaction with all three CO's, two idealized structures, C_{2v} T-shaped (**3b**) and C_{3v} trigonal pyramid (**3c**), can be envisioned for $W(CO)_3^+$. We give in Schemes 5−7 the shape of the W^+ d_π orbitals which are symmetry adapted to interact with the π^*_{CO} in each of them. Two doublet states ($^2A'$ and $^2A''$) with C_s structure resulting from a slight deformation from the idealized C_{3v} trigonal pyramid are much more strongly bound than the three doublet states with a C_{2v} T-shaped structure ($^2B_1$, $^2A_2$, $^2B_2$). In the T-shaped structure, one out of the three

SCHEME 6: Donation from a Linear Combination of σ_{CO} into an Empty W^+(5d) Orbital in Planar $W(CO)_3^+$

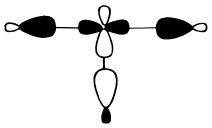

SCHEME 7: Electronic Configurations of the Back-Donating π Molecular Orbitals in the Quartet and Doublet States of Planar $W(CO)_3^+$

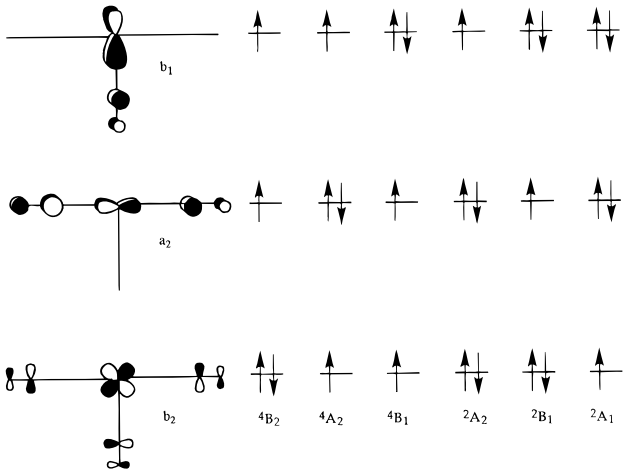

symmetry adapted linear combinations of CO lone pairs can only donate into a W^+ 6p orbital, while in the trigonal pyramid arrangement, the three symmetry adapted linear combinations of CO lone pairs can donate into the empty 6s and 5d orbitals, which are good acceptor orbitals, and some of them can also be mixed with 6p orbitals. This also explains why, on the contrary, the T-shaped arrangement of the ligands is more favorable when the W^+ electrons are quartet spin coupled: while four W^+ valence electrons can be distributed in the three d_π orbitals, the remaining fifth can be put in an sd hybrid pointing away from the ligand (i.e., along the *x* axis, see Figure 1) when the complex geometry is T-shaped, while it would have to lie in a high-energy orbital (with strong 6p character) with a trigonal pyramid structure.

In an idealized C_{3v} trigonal pyramid, the three W^+ d_π orbitals have a_1 and e symmetry, and since the a_1 has the largest overlap with the π^*_{CO} orbitals, the expected $W(CO)_3^+$ ground state derives from the $a_1^2e^3$ W^+ valence electronic configuration. The resulting doubly degenerate ^2E state splits into two states, and it leads to the $^2A'$ ground state, with the $^2A''$ state only 0.9 kcal/mol higher in energy. The Jahn−Teller distortion is indeed small since, in order to maximize metal-to-ligand π donation, ∠CWC angles are very close to 90°.

The relative energies of the three doublet T-shaped minima also derive from the relative strengths of metal-to-ligand π donation. From the shape of the three d_π orbitals given in Scheme 7, one can see that the b_2, a_2, and b_1 d_π orbitals are symmetry adapted to donate into a linear combination of three, two, and one π^*_{CO}, respectively. As expected, the $^2B_1$ state, derived from the $b_2^2a_2^2b_1^1$ electronic configuration, is the lowest one since it maximizes the W^+ to CO π donation.

We considered one T-shaped quartet structure with the electronic configuration that is expected to maximize the metal-to-ligand π donation (with two electrons in the d_π of b_2 symmetry), and the resulting $^4B_2$ state was found to be bound by 41.9 kcal/mol at the B3LYP level. We also computed a quartet state with a trigonal pyramid shape, but the extremum

SCHEME 8: Donation from Two Linear Combinations of σ_{CO} in $W(CO)_4^+$: Difference between the Square Planar and Butterfly Structures

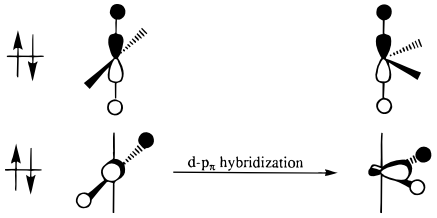

SCHEME 9: Back-Bonding π Molecular Orbitals of Butterfly $W(CO)_4^+$

found on the PES ($^4A''$) is high in energy (binding energy of 28.6 kcal/mol), and it is a transition state on the quartet PES.

$W(CO)_4^+$. Square planar (**4a** and **4b**) and butterfly (**4c**) structures have been considered for $W(CO)_4^+$. The doublet ground state has a butterfly shape, while the lowest quartet structure has a square planar geometry. As found in the cases of $W(CO)_2^+$ and $W(CO)_3^+$, the structural preference for the doublet spin state is likely to be due to the fact that, when the complex has a square planar skeleton, two linear combinations of the σ CO lone pairs can only donate into a W^+ 6p orbital, while there is only on such nonefficient σ donation scheme when the complex has a butterfly skeleton (see Scheme 8). On the contrary, a square planar geometry is more favorable for quartet states since it is possible to minimize the σ repulsion by having a W^+ valence electron along the vacant axis, while the four remaining are accommodated in the d_π ones, leading to a quartet manifold.

For the butterfly structure, we characterized the three doublet states derived from the three possible electronic configurations generated by distributing the five doublet-coupled W^+ valence electrons into the three d_π orbitals depicted in Scheme 9. The three resulting states are very close in energy (see Table 1), but still the state ordering correlates with the amounts of d_π to π^*_{CO} donation: the $^2A_1$ ground state corresponds to doubly occupying the two d_π orbitals with the largest overlap with the π^*_{CO}.

The three d_π orbitals able to donate electrons into the symmetry-adapted π^*_{CO} combinations in the idealized D_{4h} square planar geometry are given in Scheme 10. It is more favorable to maximize the occupancy of the b_{1g}, which back-donates into four CO's, rather than that of the two e_g orbitals, which only back-donate into two CO's. This leads to a $^2B_{2g}$ state with a D_{2h} minimum which has two short and two long W−C bonds (2.06 and 2.12 Å) due to the difference in W^+ to CO donation along the two metal−ligand axes. We also optimized a D_{4h} doublet state where the two e_g orbitals are both doubly occupied and the b_{1g} is singly occupied, and as expected, the corresponding $^2B_{2g}$ state is higher (by 11 kcal/mol) than the D_{2h} $^2B_{2g}$ state.

Finally, we should mention that we also optimized a $^4A_{1g}$ state with the most favorable metal-to-ligand donation scheme, and we found it to be relatively strongly bound (by 34.1 kcal/mol) at the B3LYP level. Thus the doublet/quartet energy splitting is still relatively small in $W(CO)_4^+$ (8.8 kcal/mol) and comparable to the one in $W(CO)_3^+$ (7.7 kcal/mol).

SCHEME 10: Back-Bonding π Molecular Orbitals of Square Planar $W(CO)_4^+$

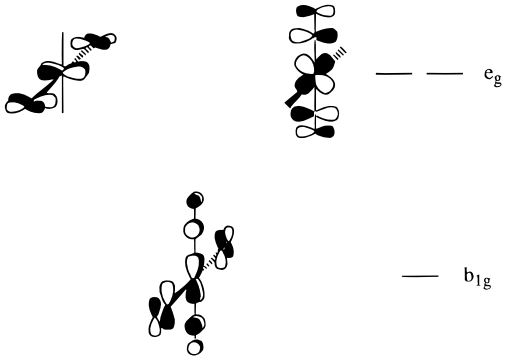

SCHEME 11: Back-Bonding π Molecular Orbitals of Square Pyramidal $W(CO)_5^+$

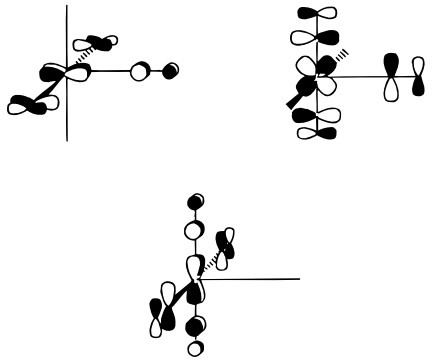

$W(CO)_5^+$. Two low-energy structures have been found on the doublet potential energy surfaces. The ground state is the $^2B_1$, and it is bound by 42.2 kcal/mol. In contrast with the smaller complexes where the quartet/doublet energy difference is small (see Table 1), the lowest quartet energy structure ($^4A_1$) lies 22.2 kcal/mol above the $^2B_1$ ground state.

Depending upon the occupation of the metal d orbitals, square pyramid and trigonal bipyramid are known to be competitive structures for pentacoordinated complexes.[26] The two doublet structures have a square pyramid geometry with a $\angle CO_{axial}-W-CO_{basal}$ angle close to 90° (see Table 1). This is already documented for other low-spin d^5 transition metal complexes.[26] We give in Scheme 11 the shape of the three d_π orbitals for a square pyramid geometry. The d_{xy} orbital can donate into the four basal CO's, while the other two only donate into the axial and two trans basal ligands. As expected, we found the $^2B_1$ ground state to be derived from the $d^2_{xy}(d_{xz}d_{yz})^3$ configuration, but there is an excited $^2B_2$ state only 4.2 kcal/mol higher in energy with a C_{4v} minimum derived from the $d^1_{xy}(d_{xz}d_{yz})^4$ electronic configuration.

We also investigated the quartet potential energy surfaces, and the two lowest states are simply derived from the two above doublet states by promoting one electron from a doubly occupied 5d into an a_1 orbital (see Table 1). We found that these $^4B_2$ and $^4A_1$ states are almost degenerate (see Table 1) at about 20 kcal/mol above the ground state. The singly occupied a_1 orbital has a strong antibonding character, which explains why these two states are high in energy.

$W(CO)_6^+$. The structure of $W(CO)_6$ in its singlet ground state is an octahedron, with the classical e_g/t_{2g} splitting of the d block. Removing an electron from one of the occupied t_{2g} orbitals leads to a Jahn−Teller distortion to a D_{4h} geometry in which two bonds, corresponding to back-donation from one singly and one doubly occupied d_π metal orbitals, are longer

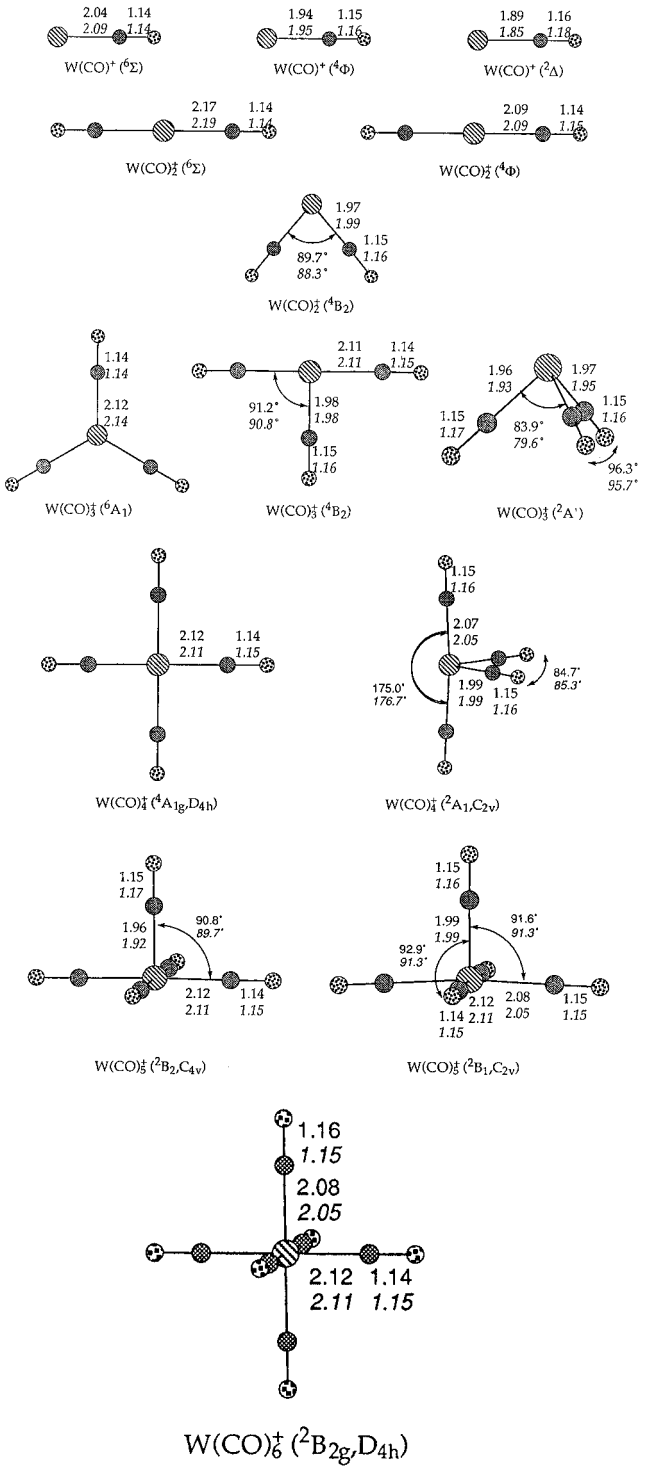

Figure 2. Comparison of the main geometrical parameters of a selected set of $W(CO)_n^+$ complexes optimized at the B3LYP/1 and MP2/1 (in italics) levels. ∠WCO, all very close to 180°, are not given in this figure.

than the other four, in which both back-donating orbitals are doubly occupied. The small magnitude of the distortion makes this structure a quasi octahedral one. Excited states arise from promotion of an electron from the t_{2g} to the e_g set (expressed in O_h symmetry) and are therefore expected to be of rather high energy.

IV. Comparison of B3LYP and *ab Initio* Results

Optimized geometries for a selected set of structures and electronic states of $W(CO)_n^+$ are shown in Figure 2. Values are given at the B3LYP/1 level, and at the MP2/1 in italics. The binding energies computed at various *ab initio* post-HF levels are presented in Table 2, where they are compared to the B3LYP results discussed in the previous section. The energetic ordering of the minima of the different PES are found to be in good agreement between *ab initio* and DFT, except for $W(CO)_2^+$ for which the former predicts the linear $^6\Sigma$ ground state and the bent $^4B_2$ state to be nearly degenerate, while B3LYP predicts the $^4B_2$ to be the ground state. Except for this case, there is no ambiguity on the spin multiplicity of the ground state: $W(CO)^+$ is a sextet, while $W(CO)_3^+$ to $W(CO)_6^+$ are doublets.

In order to obtain accurate *ab initio* D_e values for the successive metal−carbonyl binding energies, several calibration calculations were carried out using a variety of basis sets and two levels of treatment of electron correlation, MP2 and CCSD(T). The CCSD(T) level with a large basis set is expected to be reliable, but it is intractable for $W(CO)_3^+$ and larger complexes. *Ab initio* calibration calculations for $W(CO)^+$ and $W(CO)_2^+$ show the following trends (see Table 2): (i) at either the MP2 or CCSD(T) level, the use of a moderately sized basis set appears to lead to an underestimation of the binding energies (see the results obtained with basis 1 versus bases 2 and 3 in Table 2). Since a large basis set superposition error (BSSE) is expected employing such a restricted one-particle basis set in conjunction with these levels of correlation treatment, these results show the necessity to extend the one-particle basis. (ii) As expected, the correlation error is larger for a bond formation involving a spin change, leading to larger increases of BDE for the doublet than for the quartet state, itself larger than for the sextet state. The same trend is observed for larger complexes when comparing MP2 1//1 to MP2 2//2 level. (iii) It appears that the use of an f set on W (basis 2) is necessary for a good description of the bonding interaction. Since the BDE increase from basis 1 to basis 2 is fairly large, we investigated the effect of geometry reoptimization with basis 2 on several complexes in several spin states. It turned out to be negligible in all cases. (iv) For the linear states of $W(CO)^+$ and $W(CO)_2^+$, there is good agreement between the MP2 and CCSD(T) results with a given basis. Since the latter can only be performed for the smaller cases, MP2 is the method of choice for studying larger complexes, since a compromise between accuracy and tractability is unavoidable. Therefore the MP2 2//1 level was used.

Compared to B3LYP results, it is clear that MP2 2//1 BDE's are significantly larger for $W(CO)_3^+$ to $W(CO)_6^+$ (see Table 2). As can be seen in Figure 2, this is consistent with W−C bonds being shorter and C−O bonds being longer at the MP2 than at the B3LYP level. Since all of these cases correspond to doublet spin states, we expected that there was a common source of disagreement. As discussed below, experimental data in the literature show much better agreement with the B3LYP than with the MP2 results, so that additional calibration calculations at the MP2 level were performed. In particular, further basis set extensions have been investigated. We expect that this could arise from the lack of diffuse functions on C and O in our bases. In order to check this possibility, MP2 calculations were performed (using MP2/basis 1 geometries) on the linear $^6\Sigma$ states of $W(CO)^+$ and $W(CO)_2^+$ and on the bent $^4B_2$ state of $W(CO)_2^+$ with the aug-cc-pVTZ basis instead of cc-pVTZ on C and O (basis 3). The BDE of the $^6\Sigma$ state of $W(CO)^+$ is 48.2 kcal mol^{-1}, a reduction of only 0.1 kcal mol^{-1} compared to the result with basis 3. It should be noted that significant spin contamination occurs, so that the projected MP2 (PMP2) BDE is 49.4 kcal mol^{-1}. For the $^6\Sigma$ state of linear $W(CO)_2^+$, this basis set improvement does not change the computed BDE of

TABLE 2: Comparison of B3LYP and *ab Initio* Binding Energies (in kcal/mol) for a Selected Set of $W(CO)_n^+$ States

			D_e[a,b]											
			MP2							B3LYP				
				2//1		3//1		CCSD(T)				2//1	D_0 estimate	
system	structure (symmetry)	state	1//1	(diff)	2//2	(diff)	3//3	1//1	2//2	3//3	1//1	(diff)	B3LYP[c]	*ab initio*[d]
$W(CO)^+$	linear ($C_{\infty v}$)	$^6\Sigma$	41.0	47.7	47.7	48.3	48.8	41.6	47.4	46.9	53.8	54.9	51	46
				(45.2)		(48.2)						(51.9)		
	linear ($C_{\infty v}$)	$^4\Phi$	8.7	17.4	17.5	19.2	19.6	11.9	19.3	19.8	34.3			
				(13.2)										
	linear ($C_{\infty v}$)	$^2\Delta$	−21.3	−11.3	−11.2	−8.2	−7.7	−17.2	−9.2		3.4			
				(−13.7)										
$W(CO)_2^+$	linear ($D_{\infty h}$)	$^6\Sigma$	37.4	42.9	42.9	39.0	39.7	34.8	39.8		38.6	39.4	36	39
				(42.4)		(39.0)						(36.7)		
	linear ($D_{\infty h}$)	$^4\Phi$	10.0	18.9	18.9			8.3	15.5		23.8			
				(17.2)										
	bent (C_{2v})	$^4B_2$	29.7	38.0	38.0	38.9			33.8		45.8	46.9	43	38
				(36.5)		(39.2)						(44.0)		
$W(CO)_3^+$	trigonal planar (D_{3h})	$^6A_1'$	22.6	25.8								21.3		
	T-shaped (C_{2v})	$^4B_2$	35.6	44.6							41.9			
	trigonal pyramid (C_s)	$^2A'$	41.4	51.5		57.2					49.6		51	59
$W(CO)_4^+$	square planar (D_{4h})	$^4A_{1g}$	39.3	44.0	44.0						34.1			
	butterfly (C_{2v})	$^2A_1$	43.6	50.4							42.9		45	52
$W(CO)_5^+$	square pyramid (C_{2v})	$^2B_1$	48.4	53.9							42.2		43	55
	square pyramid (C_{4v})	$^2B_2$	44.0	49.0							38.0			
$W(CO)_6^+$	pseudo octahedral (D_{4h})	$^2B_{2g}$	50.3	55.8							42.0	42.0	43	55
				(54.0)										

[a] *n*//*m* stands for energy calculation with basis *n*, based on the geometry optimized using basis *m*. [b] D_e values in parentheses correspond to results obtained in the corresponding n//m basis set augmented with diffuse sp functions on CO's. [c] Corresponding to the best B3LYP calculation of D_e corrected with B3LYP/1 computed zero-point energies. [d] Corresponding to the best *ab initio* calculation of D_e corrected with B3LYP/1 computed zero-point energies.

39.0 kcal mol^{-1}. There is no significant difference with the PMP2 value of 38.8 kcal mol^{-1} in this case. Further improvement of the one particle basis was achieved by adding a supplementary p function ($\zeta = 0.06$) in the 5d region of W^+, in order to help polarize the occupied $5d_\pi$ orbitals toward the ligand(s). Again no significant change was obtained for either the $^6\Sigma$ state of $W(CO)^+$ (48.5 and 49.5 kcal mol^{-1} at the UMP2 and PMP2 levels, respectively), the $^6\Sigma$ state of linear $W(CO)_2^+$ (38.7 and 38.7 kcal mol^{-1}), or the $^4B_2$ state of bent $W(CO)_2^+$ (38.9 and 40.4 kcal mol^{-1}).

Since the worst overestimations of BDE's at the MP2 level may be on the larger complexes, calculations were performed on $W(CO)_6^+$ by enlarging the CO basis to aug-cc-pVTZ. In order to make the computation tractable, this improvement was done only for two CO ligands in trans relative positions. This energy can be compared to that of $W(CO)_4^+$ in basis 2 plus twice the energy of CO in basis 3, yielding the sum of BDE's in $W(CO)_6^+$ and $W(CO)_5^+$. The resulting value of 110.3 kcal mol^{-1} is in good agreement with the MP2 2//1 value of 109.7 kcal mol^{-1}. Therefore, the only case where basis 2 appears to be clearly insufficient is for the evaluation of the binding energy of $W(CO)_3^+$, as expected since it is associated with a spin change, leading to an large associated change in correlation energy. At this point, we have no explanation to offer for the difference in computed BDE's between B3LYP and MP2 for $W(CO)_n^+$ ($n = 3-6$).

One-particle basis set extension effects have also been investigated for the B3LYP approach (see Table 2). Indeed, Baerends and co-workers[27] recently pointed out that using a restricted basis set can lead to a substantial overestimation of the metal−ligand binding energy. Using the B3LYP/1 optimized geometries, we evaluated the effects on binding energies of (i) adding a set of f polarization functions on W^+ (B3LYP 2//1 results) and (ii) a further addition of sp diffuse functions on CO. As can be seen in Table 2, addition of f polarization functions does not change the $(CO)_5W^+-CO$ binding energy (42.0 kcal/mol) and only slightly increases the sum of the six binding energies of 281.3 instead of 276.5 kcal/mol as evaluated at the B3LYP/1 level. The same procedure also leads to a slight increase of the binding energy for W^+-CO in its $^6\Sigma$ state and $(CO)W^+-CO$ in both its $^4B_2$ and $^6\Sigma$ states (+1.1, +0.8, and +1.1 kcal/mol). Nevertheless, as can be seen in Table 2, further expansion of the basis set more than compensates this increasing effect and decreases the three above mentioned binding energies by −3.0, −2.7, and −2.9 kcal/mol, respectively. We concluded that the B3LYP/1 results are slightly overestimated but that the error is probably much smaller than that due to the neglect of spin−orbit effects.

V. Comparison to Literature Data

Comparison with Literature Values for $W(CO)_6^+$ and $W(CO)_6$. Comparison of the BDE's obtained in the present work with literature results, most of which were derived as appearance potentials in electron impact spectra, is displayed in Table 3. It can be seen that a fair agreement exists between all values for $W(CO)_4^+$ and $W(CO)_3^+$, that there is more dispersion for $W(CO)_5^+$, and that rather spectacular differences exist for $W(CO)_6^+$, $W(CO)_2^+$, and $W(CO)^+$. In the latter case most literature values, ranging from 62 to 86 kcal/mol, are unreasonably high. This is likely to be due to significant kinetic shifts, since the loss of six ligands is a relatively improbable process to occur at the threshold. The same reason could explain why our B3LYP value for the $(CO)W^+-CO$ BDE is again much lower than all measured appearance potentials of $W(CO)^+$ except that of Michels et al.[8e] There is in fact very good agreement between the latter set of experimental BDE's and our B3LYP results except for those for $W(CO)^+$.

If the maximum value of 27.7 kcal mol^{-1} from the photodissociation study by Lloyd and Schlag[1a] is corrected for the average vibrational energy of $W(CO)_6$ at 298 K of 7.5 kcal mol^{-1}, a maximum value of 35.2 kcal mol^{-1} is obtained for

TABLE 3: Bond Dissociation Energies of Tungsten Carbonyl Cations (in kcal/mol)

bond	BM[a]	FPCG[b]	WK[c]	JS[d]	MS[e]	LS[f]	this work, *ab initio*	this work, B3LYP
$(CO)_5W^+-CO$	32.1	34.8	28.6	17.8	39.0	<35.2	55	43
$(CO)_4W^+-CO$	47.7	42.7	66.9	65.5	44.3		55	43
$(CO)_3W^+-CO$	40.8	41.0	50.7	42.0	42.4		52	45
$(CO)_2W^+-CO$	48.4	57.0	62.3	51.0	51.4		59	51
$(CO)W^+-CO$	66.9	56.0	60.0	56.0	47.7		39	43
W^+-CO	69.2	48.4	62.3	86.2	61.6		46	51
sum	305.1	279.9	330.8	318.5	286.4		306	276

[a] Reference 8a. [b] Reference 8b. [c] Reference 8c. [d] Reference 8d. [e] Reference 8e. [f] Reference 1a.

$(CO)_5W^+-CO$, in acceptable agreement with the most recent appearance potential and our B3LYP value.

The sum of the six successive BDE's in $W(CO)_6^+$ can be directly obtained by another route. The heat of formation of gaseous $W(CO)_6$ at 298 K[28] is -212.0 ± 1.2 kcal mol^{-1}. On the basis of the experimental vibrational frequencies of $W(CO)_6$, its heat of formation at 0 K can be calculated at -212.9 ± 1.2 kcal mol^{-1}. The first ionization potential of gaseous $W(CO)_6$ has been determined[1a] as 8.242 ± 0.006 eV or 190.1 ± 0.1 kcal mol^{-1}. This leads to a heat of formation of $W(CO)_6^+$ at 0 K of -22.8 ± 1.3 kcal mol^{-1}. Using the 0 K heat of formation of W^+ and CO of 387 and -27.2 kcal mol^{-1},[29] the enthalpy of decomposition of $W(CO)_6^+$ into W^+ and six CO's can be estimated as 247 kcal mol^{-1}.

This amounts to the sum of the six metal−carbonyl bond enthalpies in $W(CO)_6^+$. It is noticeably smaller than the sum of B3LYP binding energies of 276 kcal mol^{-1} and even more so compared to the sum of ab initio BDE's of 306 kcal mol^{-1}. Part of the difference arises from the neglect of spin−orbit coupling in the computations. This effect is large in bare W^+, since the energy difference between the lowest ($J = {}^1/_2$) state arising from the ^{6}D ($6s^1\ 5d^4$) term and the weighted average energy of the ^{6}D is 0.514 eV or 11.9 kcal mol^{-1}.[13] In $W(CO)_6$, the t_{2g} group of orbitals splits into a $g_{3/2}^+$ of lower energy, and a doubly degenerate $e_{5/2}^+$ of higher energy. The energy gap between these two energy levels has been measured as 0.26 eV[1g] and computed as 0.23 eV.[30] If we make the assumption that this picture also holds for $W(CO)_6^+$, then two of the corresponding electrons are stabilized by ca. 0.05 eV, while the other three are destabilized by ca. 0.18 eV.[30] If we make the crude approximation that the total energy of these five electrons is the sum of the five orbital energies, this leads to an overall destabilization of ca. 0.44 eV or 10.1 kcal mol^{-1}. Adding the effects of W^+ and $W(CO)_6^+$, we obtain a decrease of the sum of BDE's in $W(CO)_6^+$ of 22 kcal mol^{-1}. This leads to satisfactory agreement between experiment and the sum of B3LYP bond energies.

We have also carried out B3LYP calculations on the neutral complexes $W(CO)_n$ ($n = 5-6$), which can be compared to experimental and previous theoretical[31a,b] results for the $(CO)_5W-CO$ BDE, and the sum of the six BDE's in $W(CO)_6$. Our estimated $(CO)_5W-CO$ BDE is 46.7 kcal mol^{-1}, in fairly good agreement with the experimental value of 46.0 ± 2 kcal mol^{-1} [31c] and previous theoretical values of 45.7[31a] and 48.0 kcal mol^{-1}.[31b] Our B3LYP optimized geometry (WC = 2.06 Å and CO = 1.16 Å) is also in excellent agreement with experiment (WC = 2.058 Å and CO = 1.148 Å).[31d] This confirms that B3LYP provides good geometries and binding energies for organometallic systems, as also found with other nonlocal density functional approaches by Ziegler et al.[31b] However, our estimated sum of the six BDE's (300.6 kcal mol^{-1}) is too large compared to the experimental value of 256 kcal mol^{-1}.[31e] This latter discrepancy might be due, as in the case of $W(CO)_n^+$, (i) to the neglect of spin−orbit effects and also (ii) to the fact that B3LYP probably does not describe accurately the differential electronic correlation between two different spin states of the system (i.e., $W(CO)_6$ and $W + 6(CO)$).

Comparison with Other Metal−Carbonyl Complexes. Comparison of the successive binding energies in $W(CO)_6^+$ to those previously determined for the carbonyl complexes of V^+,[9e] Cr^+,[9b,10a] Fe^+,[9a,10b,c,11a] Ni^+,[9d] Cu^+,[9c] and Ag^+ [9c] shows that the tungsten values are much higher than those of any of the other metals. Indeed, all values determined here at the B3LYP level lie in the 1.8−2.4 eV range (see Table 1), while the vast majority of bond energies in other cases are in the 0.5−1.5 eV range, and the largest is 1.81 eV for $NiCO^+$. The reason for these higher bond strengths cannot be attributed to a stronger electrostatic and/or polarization interaction, since the B3LYP W−C bond lengths are in the 1.95−2.08 Å range (see Table 1), while for instance the B3LYP-optimized Fe−C lengths in $Fe(CO)_n^+$ ($n = 1-5$) are slightly shorter, in the 1.89−2.04 Å range.[11a] It is likely that the additional binding strength brought about in the tungsten case is due to the better ability of its valence orbitals to hybridize for optimum interaction with the ligand orbitals. The 5s/6d mixing is very efficient due to the much better size matching between these valence orbitals in third-row metals, as compared to that in first-row metals where it is very poor.[32]

VI. Back to Chemistry

Ion−Molecule Reactions. The gas phase reactivity of $W(CO)_n^+$ ($n = 1-4$) with C_1-C_3 hydrocarbons has been shown to follow a rather complex pattern.[12] A guiding principle has been proposed,[12] according to which there must be at least two unpaired electrons on the metal for oxidative addition to proceed without a substantial activation energy. This suggests that WCO^+ (sextet) and $W(CO)_2^+$ (either quartet or sextet) should be reactive, while larger complexes should not since they all have doublet ground states with only one unpaired electron. This nicely matches experimental observations in the case of methane, since only WCO^+ and $W(CO)_2^+$ react spontaneously to form $W(CO)(CH_2)^+$ and $W(CO)_2(CH_2)^+$, respectively. However all $W(CO)_n^+$ are observed to react with larger alkanes. This can be explained as follows. The reaction of bare W^+ with methane proceeds with limited efficiency, ca. 20% of the collision rate, so that this figure is expected to be very sensitive to any change in reaction conditions, such as the presence of spectator carbonyl ligands. On the other hand, the reactions with larger alkanes are much more efficient, suggesting that the highest energy barrier and the exist channel lie significantly below the reactants' energies. Consider $W(CO)_3^+$ and $W(CO)_4^+$. Their doublet ground states are not expected to be reactive, but the transition to their lowest quartet state only requires 7.7 and 8.8 kcal mol^{-1}, respectively. Thus it is

conceivable that this transition is impossible in their reaction with methane since that of the sextet W^+ already occurs near the threshold, while it becomes accessible in the reactions with larger alkanes since they give rise to deeper initial electrostatic potential wells, and they involve metal insertion into slightly weaker C−H bonds.

Reactions with alkenes are different since simple complexation with ethene and propene is expected to be highly stabilizing. Indeed, interaction with the π bond of alkenes is qualitatively similar to that with carbonyls, with a combination of donation and back-donation. This is illustrated by the common occurrence of CO detachment in the reactions of $W(CO)_n^+$ with alkenes, a channel that is essentially absent in those with alkanes. It is therefore likely that the initial complexation of an alkene leads to a well of more than 40 kcal mol^{-1} depth (a typical tungsten−carbonyl binding energy), allowing for easy transition to states of higher spin multiplicity on the metal. This reasoning also explains why dehydrogenation of ethene and propene is spontaneous with $W(CO)_3^+$, while the only channel observed with $W(CO)_4^+$ is ligand exchange. In the former case, the initial $W(CO)_3(alkene)^+$ complex should have electronic states closely resembling those of $W(CO)_4^+$, i.e. with a small doublet-to-quartet transition energy enabling metal insertion into a C−H bond. On the contrary, the $W(CO)_4(alkene)^+$ initial complex formed with $W(CO)_4^+$ should have electronic states similar to those of $W(CO)_5^+$, in which this transition energy is much larger (34.7 kcal mol^{-1} at the B3LYP level, see Table 1).

Acknowledgment. A large part of the computations described in this paper have been carried out on the workstation cluster and Cray C98 at the Institut de Developpement et de Recherche en Informatique Scientifique (IDRIS). We thank the scientific committee of IDRIS for a generous allocation of computer resources (Project 950543).

References and Notes

(1) Some references pertaining to $W(CO)_6$ are as follows: (a) Lloyd, D. R.; Schlag, E. W. *Inorg. Chem.* **1969**, *8*, 2544. (b) Hubbard, J. L.; Lichtenberger, D. L. *J. Am. Chem. Soc.* **1982**, *104*, 2132. (c) Lichtenberger, D. L.; Kellogg, G. E. *Acc. Chem. Res.* **1987**, *20*, 379. (d) Cooper, G.; Green, J. C.; Payne, M. P.; Dobson, B. R.; Hillier, I. H. *J. Am. Chem. Soc.* **1987**, *109*, 3836. (e) Hu, Y.-F.; Bancroft, G. M.; Bozek, J. D.; Liu, Z.; Sutherland, D. G. J.; Tan, K. H. *J Chem. Soc., Chem. Commun.* **1993**, 1276. (f) Davidson, E. R.; Kunze, K. L.; Machado, F. B. C.; Chakravorty, S. J. *Acc. Chem. Res.* **1993**, *26*, 628. (g) Higginson, B. R.; Lloyd, D. R.; Burroughs, P.; Gibson, D. M.; Orchard, A. F. *J. Chem. Soc., Faraday Trans 2* **1974**, *69*, 1659.

(2) Collman, J. P.; Hegedus, L. S.; Norton, J. R.; Finke, R. G. *Principles and Applications of Organotransition Metal Chemistry*; University Science Books: Mill Valley, CA, 1987.

(3) Basolo, F. *Polyhedron* **1990**, *9*, 1503.

(4) (a) Wysocki, V. H.; Kenttämaa, H. I.; Cooks, R. G. *Int. J. Mass Spectrom. Ion Processes* **1987**, *75*, 181. (b) Horning, S. R.; Vincenti, M.; Cooks, R. G. *J. Am. Chem. Soc.* **1990**, *112*, 119.

(5) Gord, J. R.; Horning, S. R.; Wood, J. M.; Cooks, R. G.; Freiser, B. S. *J. Am. Soc. Mass Spectrom.* **1993**, *4*, 145.

(6) Beranova, S.; Wesdemiotis, C. *J. Am. Soc. Mass Spectrom.* **1994**, *5*, 1093.

(7) (a) Dejarme, L. E.; Cooks, R. G.; Ast, T. *Org. Mass Spectrom.* **1992**, *27*, 667. (b) Horning, S. R.; Kotiaho, T.; Dejarme, L. E.; Wood, J. M.; Cooks, R. G. *Int. J. Mass Spectrom. Ion Processes* **1991**, *110*, 1. (c) Riederer, D. E.; Lu, L.; Cooks, R. G. *Org. Mass Spectrom.* **1993**, *28*, 382.

(8) (a) Bidinosti, D. R.; McIntyre, N. S. *Can. J. Chem.* **1967**, *45*, 641. (b) Foffani, A.; Pignataro, S.; Cantone, B.; Grasso, F. *Z. Phys. Chem. (Munich)* **1965**, *45*, 79. (c) Winters, R. E.; Kiser, R. W. *Inorg. Chem.* **1964**, *3*, 699. (d) Junk, G. A.; Svec, H. J. *Z. Naturforsch. B* **1968**, *23*, 1. (e) Michels, G. D.; Flesch, G. D.; Svec, H. J. *Inorg. Chem.* **1980**, *19*, 479.

(9) (a) Schultz, R. H.; Crellin, K. C.; Armentrout, P. B. *J. Am. Chem. Soc.* **1991**, *113*, 8590. (b) Khan, F. A.; Clemmer, D. E.; Schultz, R. H.; Armentrout, P. B. *J. Phys. Chem.* **1993**, *97*, 7978. (c) Meyer, F.; Chen, Y.-M.; Armentrout, P. B. *J. Am. Chem. Soc.* **1995**, *117*, 4071. (d) Khan, F. A.; Steele, D. L.; Armentrout, P. B. *J. Phys. Chem.* **1995**, *99*, 7819. (e) Sievers, M. R.; Armentrout, P. B. *J. Phys. Chem.* **1995**, *99*, 8135.

(10) (a) Das, P. R.; Nishimura, T.; Meisels, G. G. *J. Phys. Chem.* **1985**, *89*, 2808. (b) Norwood, K.; Ali, A.; Flesch, G. D.; Ng, C. Y. *J. Am. Chem. Soc.* **1990**, *112*, 7502. (c) Fieber-Erdmann, M.; Holub-Krappe, E.; Bröker, G.; Dujardin, G.; Ding, A. *Int. J. Mass Spectrom. Ion Processes* **1995**, *149/150*, 513.

(11) (a) Ricca, A.; Bauschlicher, C. W. *J. Phys. Chem.* **1994**, *98*, 12899. (b) Barnes, L. A.; Rosi, M.; Bauschlicher, C. W. *J. Chem. Phys.* **1990**, *93*, 609. (c) Mavridis, A.; Harrison, J. F.; Allison, J. *J. Am. Chem. Soc.* **1989**, *111*, 2482. (d) Allison, J.; Mavridis, A.; Harrison, J. F. *Polyhedron* **1988**, *7*, 1559.

(12) Mourgues, P.; Ohanessian, G. *Rapid Commun. Mass Spectrom.* **1995**, *9*, 1201.

(13) Moore, C. E. *Atomic Energy Levels*: NSRDS-NBS Circular No. 467; U.S. GPO: Washington, DC, 1971.

(14) Stevens, P. J.; Devlin, F. J.; Chablowski, C. F.; Frisch, M. J. *J. Phys. Chem.* **1994**, *98*, 11623.

(15) Becke, A. D. *J. Chem. Phys.* **1993**, *98*, 5648.

(16) Bauschlicher, C. W., Jr.; Maitre, P. *J. Phys. Chem.* **1995**, *99*, 3444. Maitre, P.; Bauschlicher, C. W., Jr. *J. Phys. Chem.* **1995**, *99*, 6836. Holthausen, M. C.; Heinemann, C.; Cornehl, H. H.; Koch, W.; Schwarz, H. *J. Chem. Phys.* **1995**, *102*, 4931. Hack, M. D.; Maclagan, R. G. A. R.; Scuseria, E. S.; Gordon, M. S. *J. Chem. Phys.* **1996**, *104*, 6628. Barone, V.; Adamo, C.; Mele, P. *Chem. Phys. Lett.* **1996**, *249*, 290. Blomberg, M. R. A.; Siegbahn, P. E. M.; Svensson, M. *J. Chem. Phys.* **1996**, *104*, 9546.

(17) Bartlett, R. J. *Annu. Rev. Phys. Chem.* **1981**, *32*, 359.

(18) Raghavachari, K.; Trucks, G. W.; Pople, J. A.; Head-Gordon, M. *Chem. Phys. Lett.* **1989**, *157*, 479.

(19) Ross, R. B.; Powers, J. M.; Atashroo, T.; Ermler, W. C.; Lajohn, L. A.; Christiansen, P. A. *J. Chem. Phys.* **1990**, *93*, 6654.

(20) Ferhati, A.; McMahon, T. B.; Ohanessian, G. *J. Am. Chem. Soc.* **1996**, *118*, 5997.

(21) Dunning, T. H.; Hay, P. J. In *Methods of Electronic Structure Theory*; Schaefer, H. F., Ed.; Plenum Press: New York, 1977; pp 1−27.

(22) Dunning, T. H. *J. Chem. Phys.* **1989**, *90*, 1007.

(23) (a) Frisch, M. J.; Trucks, G. W.; Schlegel, H. B.; Gill, P. M. W.; Johnson, B. G.; Wong, M. W.; Foresman, J. B.; Robb, M. A.; Head-Gordon, M.; Replogle, E. S.; Gomperts, R.; Andres, J. L.; Raghavachari, K.; Binkley, J. S.; Gonsalez, C.; Martin, R. L.; Fox, D. J.; Defrees, D. J.; Baker, J.; Stewart, J. J. P.; Pople, J. A. *Gaussian 92/DFT*, Revision G.2.; Gaussian, Inc.; Pittsburgh, PA, 1993. (b) Frisch, M. J.; Trucks, G. W.; Schlegel, H. B.; Gill, P. M. W.; Johnson, B. G.; Robb, M. A.; Cheeseman, J. R.; Keith, T.; Petersson, G. A.; Montgomery, J. A.; Raghavachari, K.; Al-Laham, M. A.; Zakrzewski, V. G.; Ortiz, J. V.; Foresman, J. B.; Cioslowski, J.; Stefanov, B. B.; Nanayakkara, A.; Challacombe, M.; Peng, C. Y.; Ayala, P. Y.; Chen, W.; Wong, M. W.; Andres, J. L.; Replogle, E. S.; Gomperts, R.; Martin, R. L.; Fox, D. J.; Binkley, J. S.; Defrees, D. J.; Baker, J.; Stewart, J. J. P.; Head-Gordon, M.; Gonzales, G.; Pople, J. A. *Gaussian 94*, Revision B.3.; Gaussian, Inc.: Pittsburgh, PA, 1995.

(24) NBO version 3.1. Glendening, E. D.; Reed, A. E.; Carpenter, J. E.; Weinhold, F.

(25) Demolliens, A.; Jean, Y.; Eisenstein, O. *Organomet.* **1986**, *5*, 1457. Shen, M.; Schaefer, H. F., III; Partridge, H. *J. Chem. Phys.* **1993**, *98*, 508. Kang, S. K.; Tang, H.; Albright, T. A. *J. Am. Chem. Soc.* **1993**, *115*, 1971. Landis, C. R.; Cleveland, T.; Firman, T. K. *J. Am. Chem. Soc.* **1995**, *117*, 1859.

(26) Albright, T. A.; Burdett, J. K.; Whangbo, M. H. *Orbital Interactions in Chemistry*; John Wiley & Sons: New York, 1985.

(27) Rosa, A.; Ehlers, A. W.; Baerends, E. J.; Snijders, J. G.; te Velde, G. *J. Phys. Chem.* **1996**, *100*, 5690.

(28) (a) Barnes, D. S.; Pittam, D. A.; Pilcher, G.; Skinner, H. A.; Virmani, Y. *J. Less-Common Met.* **1974**, *36*, 177; **1974**, *38*, 53. (b) Adedeji, F. A.; Brown, D. L. S.; Connor, J. A.; Leung, M. L.; Paz Andrade, M. I.; Skinner, H. A. *J. Organomet. Chem.* **1975**, *97*, 221.

(29) Rosenstock, H. M.; Draxl, K.; Steiner, B. W.; Herron, J. T. *J. Phys. Chem. Ref. Data* **1977**, *6* (Suppl. 1).

(30) Nash, C. S.; Bursten, B. E. *New J. Chem.* **1995**, *19*, 669.

(31) (a) Ehlers, A. W.; Frenking, G. *J. Am. Chem. Soc.* **1994**, *116*, 1514. (b) Li, J.; Schreckenbach, G.; Ziegler, T. *J. Am. Chem. Soc.* **1995**, *117*, 486. (c) Lewis, K. E.; Golden, D. M.; Smith, G. P. *J. Am. Chem. Soc.* **1984**, *106*, 3905. (d) Connor, J. A. *Top. Curr. Chem.* **1977**, *71*, 71. (e) Jost, A.; Rees, B. *Acta Crystallogr.* **1975**, *B31*, 2649.

(32) Ohanessian, G.; Goddard, W. A. *Acc. Chem. Res.* **1990**, *23*, 386.